

# Mechanistic study of selective oxidation of dimethyl ether to formaldehyde over alumina-supported molybdenum oxide catalyst

Xiumin Huang, Junlong Liu, Junli Chen, Yide Xu, and Wenjie Shen\*

State Key Laboratory of Catalysis, Dalian Institute of Chemical Physics, Chinese Academy of Sciences, 457 Zhongshan Road, Dalian 116023, China

Received 11 August 2005; accepted 6 January 2006

XPS and IR spectroscopies were used to investigate the surface intermediates of dimethyl ether (DME) oxidation to formaldehyde over  $\text{MoO}_x/\text{Al}_2\text{O}_3$  catalyst. The reaction performances were tested by employing three typical reaction conditions, depending on the  $\text{O}_2$ /DME ratio and the reaction temperature. When there was sufficient oxygen present in the reaction media, a terminal or bridged  $\text{CH}_3\text{O}^*$  species formed by DME dissociation was highly active and rapidly reacted with lattice oxygen to produce formaldehyde, leading to higher selectivity of HCHO. When oxygen was consumed completely or only DME was present in the reaction media,  $\text{CH}_3\text{O}$  species bonded to more than two Mo atoms ( $\mu\text{-OCH}_3$ ) and  $\text{CH}_x$  ( $x=1\text{--}3$ ) species attached to the Mo atoms were observed and the relative ratio of ( $\mu\text{-OCH}_3$ )/Mo- $\text{CH}_x$  was significantly dependent on the reduction degree of  $\text{MoO}_x$  domains. The ( $\mu\text{-CH}_3\text{O}$ ) species was related to the formation of  $\text{CH}_3\text{OH}$  or  $\text{CO}_x$ , and the Mo- $\text{CH}_x$  species led to the formation of  $\text{CH}_4$ .

**KEY WORDS:** dimethyl ether; formaldehyde; XPS; IR;  $\text{MoO}_3/\gamma\text{-Al}_2\text{O}_3$ .

## 1. Introduction

Recent advances in the direct synthesis of dimethyl ether (DME) from synthesis gas make DME a cheaper and less toxic feedstock for the synthesis of chemicals that currently produced from methanol. Since more than half amount of methanol worldwide is used to produce formaldehyde, selective oxidation of DME to HCHO is becoming a promising alternative way [1,2].  $\text{MoO}_x$  and  $\text{VO}_x$  domains dispersed on  $\text{Al}_2\text{O}_3$  were reported to be active for DME oxidation to HCHO at low temperatures (500–550 K) with primary selectivity of 53–80%. Both DME conversion and HCHO selectivity increased with the loading of  $\text{MoO}_x$  or  $\text{VO}_x$  up to their monolayer capacities [3–5]. It was proposed that the reaction proceeds via DME dissociation followed by the oxidation step using lattice oxygen via Mars–van Krevelen redox cycles. The size of  $\text{MoO}_x$  domain governs the reaction rate by delocalizing the charge transfer related to the stabilization of the activated intermediate, and the acidity of the support controls the selectivity of products through changing the adsorption ability of the intermediates. Liu *et al.* suggested that the reaction takes place through both parallel and sequential pathways over  $\text{MoO}_x/\text{Al}_2\text{O}_3$  catalyst. HCHO and  $\text{CH}_3\text{OH}$  were the primary products, while  $\text{CO}_x$  can be produced directly by DME oxidation and indirectly by the secondary reaction of HCHO [6,7]. Our kinetic study showed that the reaction is pseudo-zero order with

respect to both dimethyl ether and oxygen molecule, suggesting that the reaction of the surface intermediate  $\text{CH}_3\text{O}^*$  is likely to be the rate-determining step [5]. DME dissociation over Mo–O sites was recently investigated by  $^{18}\text{O}$  and H–D isotopic tracers and it was revealed that the oxy-dehydrogenation of  $\text{CH}_3\text{O}^*$  could not be the rate-determining step [8]. The HCHO/ $\text{CH}_3\text{OH}$  ratio in the products was closely related to the concentrations of DME and  $\text{O}_2$  in a certain range in the feed stream. Lower DME pressure and higher  $\text{O}_2$  pressure favored the formation of formaldehyde with a higher ratio of HCHO to  $\text{CH}_3\text{OH}$ .

In the present work, we investigated the surface changes of the  $\text{MoO}_3/\text{Al}_2\text{O}_3$  catalyst with respect to the  $\text{O}_2$ /DME feed ratio. The catalysts were characterized by XPS and *in situ* IR techniques. The results were correlated with the catalytic performance at the same  $\text{O}_2$ /DME feed ratio, and the possible reaction pathway of DME selective oxidation to HCHO was proposed accordingly.

## 2. Experimental

### 2.1. Catalyst preparation

A 30 wt%  $\text{MoO}_3/\text{Al}_2\text{O}_3$  (ca. 5.5 Mo atoms/ $\text{nm}^2$  at the monolayer coverage, and hereafter denoted as 30 $\text{MoO}_3/\text{Al}_2\text{O}_3$ ) catalyst was prepared by the wet-impregnation of a commercially available  $\gamma\text{-Al}_2\text{O}_3$  (BET surface area of 227  $\text{m}^2/\text{g}$ ) with an aqueous solution of ammonium heptamolybdate  $((\text{NH}_4)_6\text{Mo}_7\text{O}_{24}\cdot 4\text{H}_2\text{O})$ . The obtained

\* To whom correspondence should be addressed.  
E-mail: shen98@dicp.ac.cn

sample was dried at 373 K overnight and calcined at 773 K for 3 h in air.

## 2.2. DME oxidation

The selective oxidation of DME was carried out in a continuous-flow fixed-bed quartz reactor in the temperature range of 543–573 K under atmospheric pressure. About 50 mg catalyst sample was diluted with 200 mg quartz powder to prevent the temperature gradients in the catalyst bed and was charged into the reactor. Two premixed gases of 10.15% DME/He and 9.95% O<sub>2</sub>/He were introduced through two parallel mass flow controllers, respectively, and the O<sub>2</sub>/DME ratio was adjusted in the range of 0–0.36 in the reaction stream. The reactor effluents were analyzed by an online gas chromatograph equipped with TCD and FID detectors. A TDX-01 and Porapak Q combined packed column was used for the separation of O<sub>2</sub>, N<sub>2</sub>, CO, CO<sub>2</sub>, H<sub>2</sub>O, HCHO, CH<sub>3</sub>OH and DME. A PLOT Q capillary column connected to the FID detector was used for the separation and detection of CH<sub>4</sub>, C<sub>2</sub>H<sub>4</sub>, CH<sub>3</sub>OH, DME, and methyl formate (MF).

## 2.3. XPS spectroscopy

The XPS spectra were recorded at room temperature using an AMICAS spectrometer (KROTAS instrument, Shimadzu) with Mg K<sub>α</sub> radiation ( $h\nu = 1253.6$  eV). Powder of the 30MoO<sub>3</sub>/Al<sub>2</sub>O<sub>3</sub> catalyst was pressed into pellet and mounted on a quartz cell. The sample was first heated to a desired temperature in He flow (35 mL/min), and the DME/O<sub>2</sub>/He gas mixture was then introduced into the cell. After 30 min reaction, the samples were cooled down to room temperature under He flow and transferred into the analysis chamber without exposure to air.

Al2p (74.5 eV) level of the  $\gamma$ -Al<sub>2</sub>O<sub>3</sub> carrier was taken as an internal reference [9]. A Shirley background subtraction was applied and Gauss–Lorentz (85:15) curves were used for the curve-fitting. During the deconvolution of the XPS spectrum of Mo species, the full widths at half maximum (FWHM) of Mo3d<sub>3/2</sub> and Mo3d<sub>5/2</sub> are taken the same value and the peak area ratio of Mo3d<sub>5/2</sub>:Mo3d<sub>3/2</sub> is equal to 3:2. The value of the FWHM of the C1s spectra for CH<sub>3</sub>O species and C1s for CH<sub>x</sub> species were taken the same. All the signal intensities were normalized using the relative sensitivity factors (RSF) of 0.257, 0.318, 3.585 and 0.736 for Al2p, C1s, Mo3d and O1s, provided by the instrument manufacturer.

Peak broadening of the Mo species were also evaluated by comparing the FWHM ratios of Mo to that of the Al species to eliminate the incoherent peak-width of the same element at different tests.

## 2.4. In situ FT-IR spectroscopy

The FT-IR spectra were collected over a Biorad Vector 22 spectrometer equipped with a DTGS detector

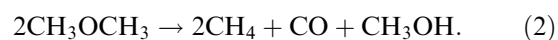
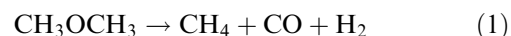
at a resolution of 4 cm<sup>-1</sup>. The catalyst was pressed into a thin self-supporting wafer and placed inside of a heatable IR cell with ZnSe windows. It was first treated with He stream at 723 K for 1 h to remove the adsorbed water. Then, the sample was oxidized with 10% O<sub>2</sub>/He at 573 K for 0.5 h, and the background was recorded after flushing the treated sample with He for about 0.5 h.

Pure DME was introduced into the IR cell at 523 and 573 K, respectively. Physically adsorbed DME molecules were removed by flushing with He for 0.5–1 h at the same adsorption temperature before the corresponding IR spectra were recorded.

## 3. Results and discussion

### 3.1. Catalytic evaluation

DME oxidation reactions over the MoO<sub>3</sub>/Al<sub>2</sub>O<sub>3</sub> catalyst were performed at 543 and 573 K by varying the O<sub>2</sub>/DME ratio of 0–0.36 in the feed stream. The reaction results are summarized in table 1. When only DME was fed at 573 K, DME conversion only reached 0.4%, and the major products were CH<sub>4</sub>, CO, CH<sub>3</sub>OH with a little amount of CO<sub>2</sub> and traceable C<sub>2</sub>H<sub>4</sub>. No formaldehyde could be detected. By comparing the relative concentration of CH<sub>4</sub>, CO<sub>x</sub> and CH<sub>3</sub>OH, it can be found that the decomposition of DME was not consistent exactly with reaction equation (1), and it seems to be a combination of equations (1) and (2) with CH<sub>4</sub> as the dominant product.



When oxygen was added into the feedstock, the formation of formaldehyde became the domain reaction, which was dependent on the reaction temperature and the O<sub>2</sub>/DME ratio. When the reaction was performed at 543 K with O<sub>2</sub>/DME ratio of 0.16, DME conversion was 6.3% and only ca. 33% of the oxygen was consumed, indicating that the reaction was under oxygen-rich condition. HCHO and CO were obtained as the major products with selectivities of 54.9% and 37.6%,

Table 1  
Effect of O<sub>2</sub>/DME ratio on the product selectivity of DME oxidation over 30MoO<sub>3</sub>/Al<sub>2</sub>O<sub>3</sub> catalyst

O <sub>2</sub> /DME	Temp (K)	Conversion %				Product selectivity %			
		O <sub>2</sub>	DME	CO <sub>2</sub>	CO	HCHO	CH <sub>3</sub> OH	MF	CH <sub>4</sub>
0	573	0	0.40	9.58	26.85	0	16.79	0	46.78
0.16	543	32.6	6.31	3.06	37.58	54.9	3.72	0.73	0
0.16	573	100	11.62	1.72	38.79	52.65	6.06	0.79	0.11
0.36	573	72.9	17.25	2.54	45.72	49.67	1.88	0.18	0

respectively. No  $\text{CH}_4$  was formation was observed. With further increasing the reaction temperature up to 573 K, oxygen in gas phase was consumed completely, and thus the reaction was carried out under oxygen-deficient condition. The DME conversion approached to about 12%, and the selectivity of HCHO slightly decreased to 52.7%, whereas the selectivities of  $\text{CH}_3\text{OH}$  and CO increased marginally. However, traceable  $\text{CH}_4$  was detected in the tail-gas with a selectivity of 0.11%. When the  $\text{O}_2/\text{DME}$  ratio was increased to 0.36 at 573 K, it was found that 73% of oxygen was consumed and thus the reaction was carried out under oxygen-rich condition. The selectivity toward HCHO decreased to 49.7% and the selectivity of CO increased to 45.7%. Noticeably, no  $\text{CH}_4$  production could be detected, which is similar to the case of  $\text{O}_2/\text{DME}=0.16$  at 543 K.

It seems that the selectivities of HCHO and CO during DME oxidation of DME over the  $\text{MoO}_3/\text{Al}_2\text{O}_3$  catalyst are not remarkably dependent on the reaction temperature and the  $\text{O}_2/\text{DME}$  ratio. But the formation of methane is closely related to the presence of oxygen in the reaction media, that is, whether the reaction was carried out under oxygen-rich or oxygen-deficient atmosphere.

### 3.2. XPS characterization of the used catalysts

Prior to the XPS measurements, the catalyst was treated at the following reaction conditions in the fixed-bed reactor. (1)  $\text{O}_2/\text{DME}=0.16$  at 543 K, i.e. excessive  $\text{O}_2$  was present, and there was no methane formation. There was no deactivation occurred during 17h time on stream; (2)  $\text{O}_2/\text{DME}=0.16$  at 573 K, i.e. gaseous  $\text{O}_2$  were completely consumed, and the formation of methane took place. The reaction could last for 2 h without any changes in catalytic performance and fol-

lowed by slight deactivation with time on stream; (3) only DME was fed at 573 K, methane was formed as the main product through the decomposition of DME. The conversion of DME decreased from 0.57% to 0.34% after running the reaction for 2.5 h, indicating slight deactivation of the catalyst. Therefore, the following XPS measurements were conducted over the catalysts, which were tested in the quartz cell of the XPS chamber for 30 min under the reactions conditions as described above.

Figure 1 shows the XPS spectra of C1s, O1s and Mo3d in the fresh and the used  $\text{MoO}_3/\text{Al}_2\text{O}_3$  catalysts, and the surface compositions of each component are summarized in table 2. For the case of  $\text{O}_2/\text{DME}=0.16$  at 543 K, under which excessive  $\text{O}_2$  was present in the reaction media, no change could be observed in the XPS spectra of O1s, C1s and Mo3d when compared with the fresh catalyst. The O1s spectrum showed a unique peak at binding energy of 531.3 eV, which could be attributed to the lattice oxygen of both  $\text{Al}_2\text{O}_3$  (531.1–531.4 eV) and  $\text{MoO}_3$  (530.62 eV). Overlapping contribution from molybdenum often made it difficult to discriminate the different oxygen peaks in the monolayer  $\text{MoO}_3/\text{Al}_2\text{O}_3$  catalyst [10]. The intensity of contaminated C1s signal was almost the same as the fresh sample. This may suggest that no surface carbonaceous species were formed, namely, the reactant (DME) and the product (HCHO) did not give rise to any carbon-containing signal on the catalyst surface. Meanwhile, the Mo species in the catalyst still remained unreduced, indicating that the presence of oxygen in the gas phase kept the high oxidation state of the surface molybdenum atoms. Similar phenomena were observed in the case of  $\text{O}_2/\text{DME}=0.36$  at 573 K, no remarkable changes in the O1s, C1s and Mo3d spectra took place as compared with the fresh catalyst.

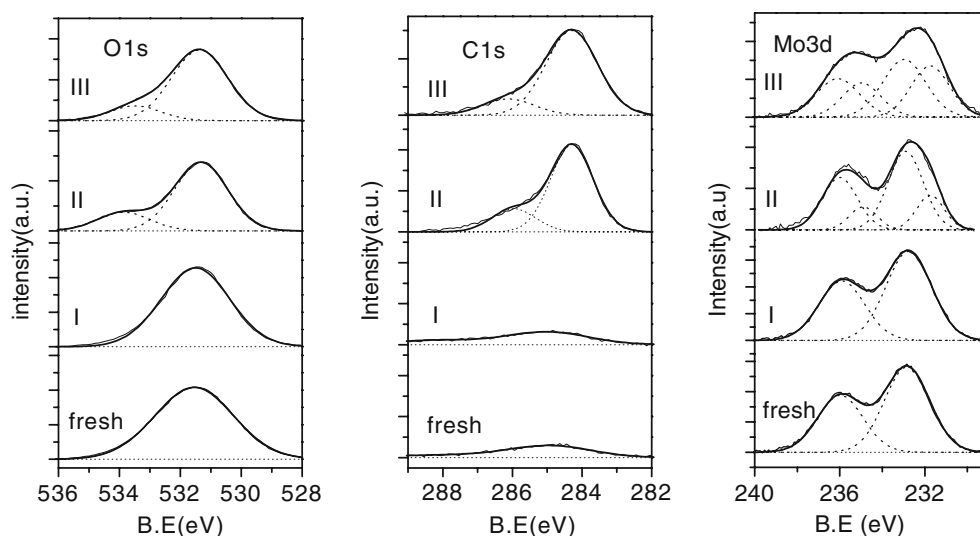
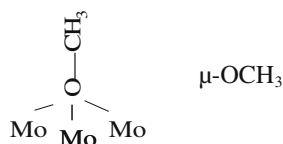


Figure 1. O1s, C1s, and Mo3d spectra of the fresh and used catalysts. • Reaction conditions: (I)  $\text{O}_2/\text{DME} = 0.16$ ,  $T = 543$  K; (II)  $\text{O}_2/\text{DME} = 0.16$ ,  $T = 573$  K; (III) Only DME,  $T = 573$  K.

Table 2  
The surface compositions of C1s, O1s, and Mo3d in the fresh and used catalysts

Reaction condition	C1s		O1s		B.E. (eV)		Mo(VI) %	FWHM	Surface Mo/Al ratio
	CH <sub>3</sub> %	CH <sub>3</sub> O %	Lattice O %	CH <sub>3</sub> O %	Mo <sub>3d5/2</sub>	Mo <sub>3d3/2</sub>			
Fresh	0	0	100	0	232.8	235.9	100	1.00	0.1393
O <sub>2</sub> /DME=0.16, 543 K	0	0	100	0	232.8	235.9	100	1.177	0.1808
O <sub>2</sub> /DME=0.16, 573 K	75.5	24.5	78.5	21.5	232.6	235.7	74.5	1.353	0.1803
DME, 573 K	84.4	15.6	80.6	19.4	232.4	235.5	54.7	1.459	0.1801

When the catalyst was treated with O<sub>2</sub>/DME=0.16 at 573 K, in which the oxygen in gas phase was completely consumed, two distinct O1s peaks were observed at 531.3 and 533.6 eV, respectively. The binding energy at 531.3 eV can be easily assigned to the lattice oxygen of Al<sub>2</sub>O<sub>3</sub> and MoO<sub>3</sub>, while the determination of the binding energy at 533.6 eV is somewhat difficult. The assignment of the component to adsorbed –OH (H<sub>2</sub>O) [11] or HCHO could be first excluded. H<sub>2</sub>O and HCHO was also formed over the catalyst treated by O<sub>2</sub>/DME=0.16 at 543 K, but no O1s peak at 533.6 eV was observed. Similar O1s peak at 533.6 eV during methanol adsorption on ZnO surface was previously observed and attributed to the formation of CH<sub>3</sub>O species [12]. Hence, the new O1s peak at 533.6 eV could be assigned to CH<sub>3</sub>O-species attached to Mo, probably bounded to multiple Mo ions (denoted as  $\mu$ -OCH<sub>3</sub>) as revealed by our IR spectroscopy experiments in Section 3.4. Briand *et al.* also inferred that one molecule of methanol could form one surface methoxy connected with 3–4 Mo atoms on polymerized surface molybdenum oxide [13].



Scheme 1. Possible reactive pathway of DME oxidation.

The newly formed  $\mu$ -OCH<sub>3</sub> species can be further confirmed by the corresponding C1s spectrum. The C1s peak displayed two components with binding energies of 284.3 and 286.0 eV, respectively. The band at 284.3 eV corresponds to hydrocarbon species CH<sub>x</sub> ( $x=1-3$ ), probably in the form of Mo–CH<sub>x</sub> ( $x=1-3$ ). The band at 286.0 eV corresponds to the formation of methoxy species, probably in the form of  $\mu$ -OCH<sub>3</sub> [12,14–18]. Simultaneously, Mo was partially reduced with ca. 74.5% of Mo (6+) species remained, and the binding energy shifted from 232.8 eV to 232.6 eV and the relative FWHM of Mo to Al increased from 1.18 to 1.35.

When only DME was introduced over the MoO<sub>3</sub>/γ-Al<sub>2</sub>O<sub>3</sub> catalyst at 573 K, two kinds of carbo-

naceous species were also formed. However, the ratio of Mo–CH<sub>x</sub>/μ-CH<sub>3</sub>O calculated from the C1s spectra was much higher than that as observed in the case of O<sub>2</sub>/DME = 0.16 at 573 K, and the concentration of μ-OCH<sub>3</sub> species decreased from 24.5% to 15.6%. The binding energy of Mo3d peak shifted to much lower values and the relative FWHM ratio of Mo/Al further increased to 1.46. This means that Mo species was reduced to a greater extent with only 54.7% of Mo (6+) species left.

The surface Mo/Al ratio increased from 0.14 of the fresh catalyst to 0.18 after DME oxidation reactions. This indicates that the large oxo-anions of MoO<sub>x</sub> domains would break into smaller structures and yield well-dispersed molybdenum oxide phases. This kind MoO<sub>x</sub> species enrichment on the surface was also previously reported by Damyanova *et al.* [19].

### 3.3. XPS spectra of DME adsorption

Figure 2 shows the XPS spectra of C1s, O1s and Mo3d after DME adsorption at different temperatures for 30 min. The catalyst was pre-oxidized at 573 K for 0.5 h before DME adsorption. Table 3 listed the deconvoluted results of C1s and Mo3d. The C1s intensity for pre-oxidized sample was subtracted as background from each spectrum to obtain the intrinsic intensities of the adsorbed species.

The intensity of C1s after adsorption of DME at 293 K was a little higher than that of the pre-oxidized one. This indicated that chemical adsorption of DME were negligible at room temperature. The ratio of CH<sub>3</sub>O/CH<sub>3</sub> equals to 1, suggesting that the oxydehydrogenation of CH<sub>3</sub>O\* species did not happen. When temperature increased up to 488 K, DME chemisorption occurred with the Mo3d peak shifting to 232.5 eV, implying the partial reduction of Mo<sup>6+</sup> took place. The C1s peak displayed three components with binding energies of 284.3 eV for CH<sub>x</sub> ( $x=1-3$ ), 286.2 eV for CH<sub>3</sub>O-(μ-OCH<sub>3</sub>) and 288.3 eV for carbonate [12,14–18]. The O1s peak showed two types of oxygen species, i.e. B.E=531.4 eV and 533.4 eV. The binding energy at 531.4 eV was due to the lattice oxygen of Al<sub>2</sub>O<sub>3</sub> and MoO<sub>3</sub>, and the binding energy at 533.4 eV represented the oxygen from the μ-CH<sub>3</sub>O species.

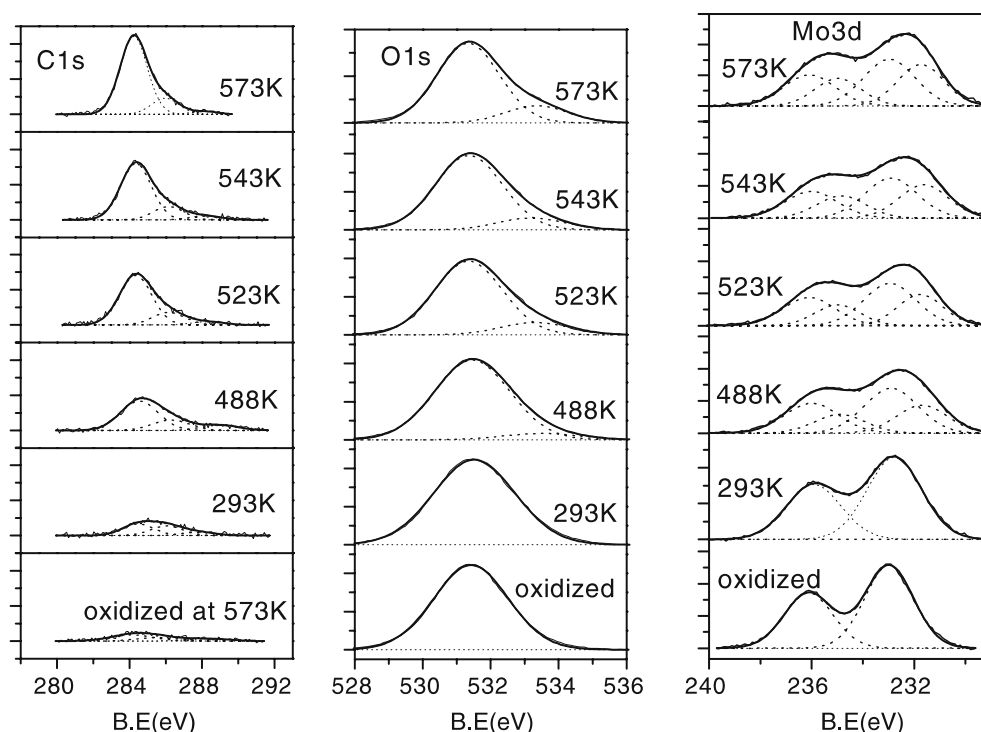


Figure 2. The C1s, O1s, and Mo3d spectra recorded after DME adsorption at different temperatures for 30 min.

Table 3  
DME adsorption over the  $\text{MoO}_3/\text{Al}_2\text{O}_3$  catalyst

Temperature, K	Deposited C*	C1s			Mo3d	
		$\text{CH}_x$ %	$\text{CH}_3\text{O}$ %	$\text{CO}_3^{2-}$ %	Mo(VI) %	Mo(V) %
Pre-oxidized	1				100	0
293	1.59	50	50	0	100	0
488	3.40	72.9	21.3	5.7	59.9	40.1
523	4.44	80.0	17.4	2.7	60.3	39.7
543	4.55	83.8	15.0	1.4	57.2	42.8
573	7.19	87.4	12.6	0	54.7	45.3

\* Relative area of C deposit to pre-oxidized.

It can be further seen from table 3, both the amount of adsorbed carbon species and the ratio of  $\text{Mo}-\text{CH}_x/\mu\text{-CH}_3\text{O}$  increased with temperature. The percentage of  $\mu\text{-CH}_3\text{O}^*$  species decreased from 21.3% at 488 K to 12.6% at 573 K. On the other hand, the content of  $\text{Mo}^{5+}$  increased from 40% at 488 K to 45.3% at 573 K. This means that the dissociative adsorption of DME was accompanied by the dissociated  $\text{CH}_3\text{O}^*$  species reacting with the lattice oxygen, resulting in the partial reduction of  $\text{Mo}^{6+}$ .

### 3.4. FT-IR characterization of DME adsorption on the $\text{MoO}_x/\text{Al}_2\text{O}_3$ catalyst

Figure 3 shows the FT-IR spectra of DME adsorption on the  $\text{MoO}_x/\text{Al}_2\text{O}_3$  catalyst at 523 K. Obviously,

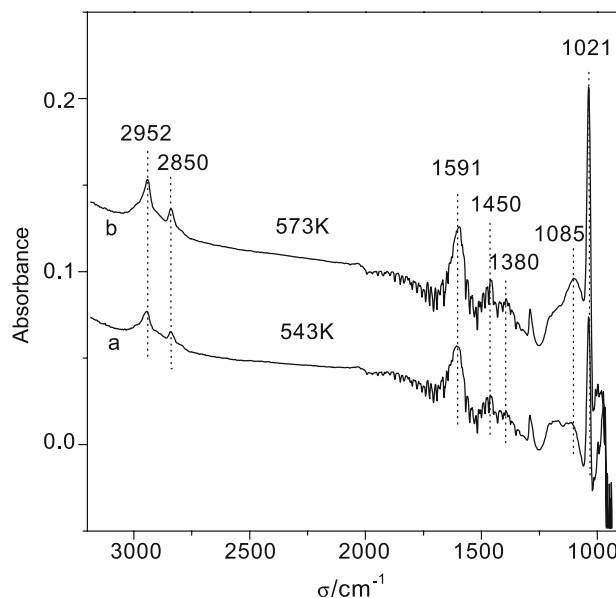


Figure 3. IR spectra of DME adsorption at 523 and 573 K. (a) 523 K, flushed with he for 30 min; (b) 573 K, flushed with he for 30 min.

DME adsorption led to the appearance of the bands at 1021, 1450, 1380 and 1278  $\text{cm}^{-1}$  in addition to the bands of C–H stretching at 3000–2800  $\text{cm}^{-1}$ . The sharp band at 1021  $\text{cm}^{-1}$  could be attributed to  $\nu(\text{CO})$  of the  $\mu\text{-OCH}_3$  species bounded to multiple Mo ions [20,21]. The bands at 2848 and 2952  $\text{cm}^{-1}$  corresponded to the symmetric bend ( $2\delta_s$ ) and the symmetric C–H stretch ( $\nu_s$ ) of the  $\text{CH}_3$  in adsorbed surface methoxy species, respec-

tively [13,22]. Although the reduced nature of Mo may cause the C–H stretching bands of the  $\text{CH}_3\text{O}$  species shift to lower frequencies [23], it was still higher than the C–H bands at 2931 and 2831  $\text{cm}^{-1}$  in the selective oxidation of  $\text{CH}_3\text{OH}$  over  $\text{V}_2\text{O}_5/\text{Al}_2\text{O}_3$  catalyst [22]. It was previously observed that the C–H stretching frequencies of the  $\text{CH}_3\text{O}$  species formed by DME adsorption were higher than those by  $\text{CH}_3\text{OH}$  adsorption on  $\text{ZrO}_2$  support [24]. This suggests that the C–H bond of the  $\text{CH}_3\text{O}$  species generated by DME adsorption is stronger than that by  $\text{CH}_3\text{OH}$ . The bands at 1450 and 1380  $\text{cm}^{-1}$  can be assigned to the  $\text{CH}_3$  deformation ( $\delta(\text{CH}_3)$ ) vibration of the methoxy species or to the  $\nu(\text{OCO})$  vibration of formate and unidentate carbonate [20]. The bands at 1591  $\text{cm}^{-1}$  can be attributed to the hydroxyl group of water. When the adsorption temperature was increased to 573 K, the IR spectra were almost the same as recorded at 523 K, but the corresponding intensities became stronger. This indicates that more carbonaceous species were formed on the catalyst surface as the adsorption temperature increased.

Figure 4 shows the band intensity changes of the  $\mu\text{-CH}_3\text{O}$  at 1021  $\text{cm}^{-1}$  when it was treated with 10%  $\text{O}_2/\text{He}$  at different temperatures and durations. It was found that the  $\mu\text{-CH}_3\text{O}$  species formed after DME adsorption at 573 K was rather stable and began to react with oxygen at 473 K. The intensity of the band at 1021  $\text{cm}^{-1}$  decreased with increasing the oxidation temperature and it was completely vanished at 573 K.

#### 4. Possible reactive intermediates of DME oxidation

The formation of  $\text{CH}_x\text{-Mo}$  and  $\mu\text{-CH}_3\text{O}^*$  species as characterized by XPS and IR techniques demonstrates

that the dissociation of  $\text{CH}_3\text{OCH}_3$  on  $\text{MoO}_x$  surfaces happened at higher temperatures. In case of oxygen-rich in the reaction media ( $\text{O}_2/\text{DME} = 0.16$  at 543 K), no surface carbonaceous species were formed. This implied that the  $\text{CH}_3\text{O}^*$  species (hereafter denoted as  $\alpha\text{-CH}_3\text{O}$ ) formed from DME dissociation on  $\text{MoO}_x/\text{Al}_2\text{O}_3$  catalyst was highly reactive, and it may react immediately with the lattice oxygen on the catalyst surface to produce formaldehyde. Therefore, the  $\alpha\text{-CH}_3\text{O}$  species could not be detected by XPS technique. Meanwhile, the produced  $\text{HCHO}$  was weakly adsorbed on the surface and could be desorbed easily, thus the secondary reactions was avoided and led to higher selectivity of formaldehyde. This can also be proved by the corresponding IR spectra (figure 5). The C=O stretching at 1772 and 1746  $\text{cm}^{-1}$  of the produced  $\text{HCHO}$  [25] was observable during the reaction, however, these bands disappeared after flushing with a He stream for 0.5 h.

Previous IR studies of DME adsorption over  $\text{ZrO}_2$  indicated the presence of terminal (*t*-) and bridged (*b*-)  $\text{CH}_3\text{O}$  species [24]. DME adsorption at 573 K presented the C=O stretching bands ( $\nu\text{CO}$ ) at 1145 and 1040  $\text{cm}^{-1}$  due to the formation of *t*- $\text{OCH}_3$  and *b*- $\text{OCH}_3$  species. The weak mobility of the lattice oxygen of  $\text{ZrO}_2$  made the produced *t*- $\text{CH}_3\text{O}$  and *b*- $\text{CH}_3\text{O}$  stable even at 573 K. Very weak C=O stretching band of  $\text{CH}_3\text{O}$  species at 1065 and 1150  $\text{cm}^{-1}$  on the selective oxidation of  $\text{CH}_3\text{OH}$  under oxygen-rich conditions was also observed over vanadia/alumina catalyst [22,26], suggesting that the  $\text{CH}_3\text{O}^*$  species produced was in a terminal and bridged form [19,24]. So the  $\alpha\text{-CH}_3\text{O}$  species attached to the unreduced Mo ions is most likely to be terminal or bridged  $\text{CH}_3\text{O}$  under oxygen-rich conditions, acting as the active intermediate for  $\text{HCHO}$  formation in the present case. The corresponding reaction

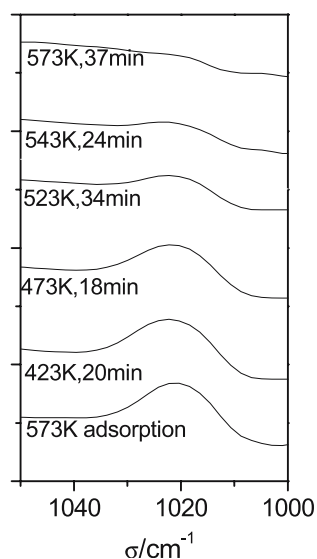


Figure 4. Temperature dependence of the intensity of the IR band at 1021  $\text{cm}^{-1}$  of the  $\mu\text{-CH}_3\text{O}$  species.

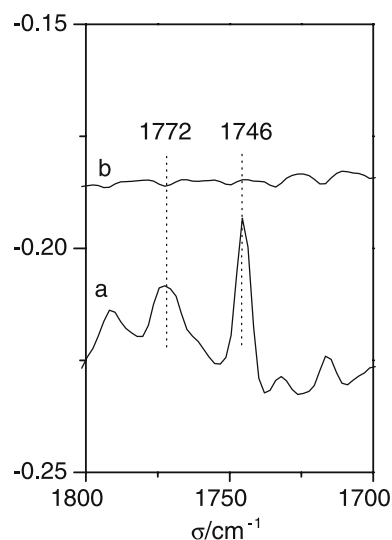
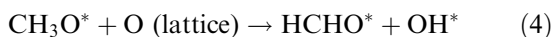
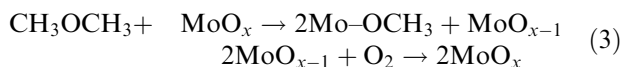


Figure 5. IR spectra of produced  $\text{HCHO}$ . (a) DME oxidation process at 573 K (b) He flush for 30 min at 573 K.

tests also showed that no  $\text{CH}_4$  formation could be detected because of the absence of  $\text{CH}_x$  species.

DME dissociation over  $\text{MoO}_x$  domain would generate  $\alpha\text{-CH}_3\text{O}^*$  species and caused the partial reduction of  $\text{MoO}_x$  species according to equation [3], but re-oxidation of the reduced molybdenum by gaseous oxygen occurred simultaneously and maintained the high oxidation state of the surface molybdenum atoms. This would favor the formation of  $\text{HCHO}$  and inhibit  $\text{CH}_3\text{OH}$  formation through the competition of the following surface reactions (4) and (5):

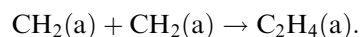
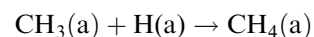


This is consistent with the results reported for propane oxidative dehydrogenation with *in situ* Raman-GC technique by Mul *et al.* who concluded that the vanadia/alumina catalyst was essentially in oxidized states under oxygen-rich conditions [27].

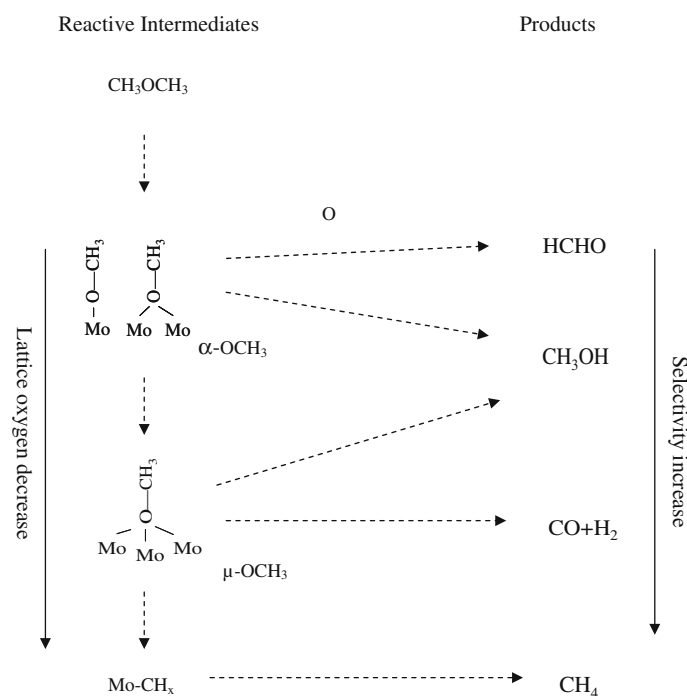
In the case of oxygen-deficient in the reaction media ( $\text{O}_2/\text{DME}=0.16$  at 573 K), the dissociated  $\text{CH}_3\text{O}$  species reacted with lattice oxygen, resulting in the reduction of surface molybdenum and the formation of  $\mu\text{-OCH}_3$  and  $\text{Mo-CH}_x$  species, as revealed by XPS measurements. FT-IR study on high temperature DME adsorption over  $\text{CeO}_2$  suggested that the precursor of the  $\mu\text{-OCH}_3$  was the bridged- $\text{OCH}_3$  rather than the

terminal- $\text{OCH}_3$ , and  $\mu\text{-OCH}_3$  remained on the surface after the terminal or bridged- $\text{OCH}_3$  disappeared [20].

DME oxidation at  $\text{O}_2/\text{DME}=0.16$  and 573 K showed that the selectivity of  $\text{CH}_3\text{OH}$  and  $\text{CO}$  increased and the selectivity to  $\text{HCHO}$  slightly decreased with the formation of traceable of  $\text{CH}_4$ . Combining the reaction behavior with the surface states revealed by XPS measurements, it is reasonable to say that the  $\mu\text{-OCH}_3$  species attached to the reduced Mo was responsible for the formation of  $\text{CH}_3\text{OH}$  and/or  $\text{CO}$ , while the  $\text{Mo-CH}_x$  species should be related to the formation of  $\text{CH}_4$ . The more the reduced vacancies on the catalyst surface, the stronger the C-O bond and the weaker the C-H bond of methoxy species on molybdenum oxide, and thus more  $\text{CO}$  would be formed [28]. The formation of  $\text{CH}_4$  can be described by the following routes.



When only DME was fed, the lattice oxygen further decreased due to the deeper reduction of Mo species, resulting in a higher ratio of  $\text{Mo-CH}_x/\mu\text{-CH}_3\text{O}$ . Consequently, the selectivity of  $\text{CH}_4$  was significantly increased. This gives further evidence that  $\text{CH}_x$  should be related to the formation of  $\text{CH}_4$ , and the formation of  $\text{CH}_3\text{OH}$  and  $\text{CO}$  may be originated from the  $\mu\text{-OCH}_3$  species formed. Therefore, the reaction pathway of the selective oxidation of DME may be proposed as follows:



Scheme 2.

## 5. Conclusions

Dissociative adsorption of DME over  $\text{MoO}_3/\text{Al}_2\text{O}_3$  catalyst was found to be dependent on the  $\text{O}_2/\text{DME}$  ratio and the reaction temperature. When there was sufficient oxygen present in the reaction media, the dissociated  $\alpha\text{-CH}_3\text{O}^*$  (terminal or bridged  $\text{CH}_3\text{O}$ ) was highly active and immediately reacted with the lattice oxygen to produce  $\text{HCHO}$ , leading to higher selectivity of formaldehyde. When oxygen was consumed completely or only DME was present in the reaction media,  $\text{CH}_3\text{O}$  species bonded to more than two Mo atoms ( $\mu\text{-OCH}_3$ ) and  $\text{CH}_x$  species attached to the reduced Mo atoms were observed and the relative ratio of  $\mu\text{-OCH}_3/\text{Mo-CH}_x$  was significantly dependent on the reduction degree of  $\text{MoO}_x$  domains. The  $\mu\text{-CH}_3\text{O}$  species was related to the formation of  $\text{CH}_3\text{OH}$  or  $\text{CO}_x$ , and the  $\text{Mo-CH}_x$  species led to the formation of  $\text{CH}_4$ .

## Acknowledgments

This work was supported by the National Natural Science Foundation of China (20473087).

## References

- [1] J.L. Li, X.G. Zhang and T. Inui, *Appl. Catal. A* 147 (1996) 23.
- [2] G.Y. Cai et al., *Appl. Catal. A* 125 (1995) 29.
- [3] H.C. Liu and E. Iglesia, *J. Catal.* 208 (2002) 1.
- [4] H.C. Liu, P. Cheung and E. Iglesia, *Phys. Chem. Chem. Phys.* 5 (2003) 3795.
- [5] X.M. Huang, Y.G. Li, Y.D. Xu and W.J. Shen, *Catal. Lett.* 97(3–4) (2004) 185.
- [6] H.C. Liu, P. Cheung and E. Iglesia, *J. Catal.* 217 (2003) 222.
- [7] H.C. Liu, P. Cheung and E. Iglesia, *J. Phys. Chem. B* 107 (2003) 4118.
- [8] P. Cheung, H.C. Liu and E. Iglesia, *J. Phys. Chem. B* 108 (2004) 18650.
- [9] J. Sarrín, O. Noguera, H. Royo, M.J. Pérez Zurita, C. Scott, M.R. Goldwasser, J. Goldwasser and M. Houalla, *J. Mol. Cat. A: Chem.* 144 (1999) 441.
- [10] B.M. Reddy, B. Chowdhury, E.P. Reddy and A. Fernández, *Appl. Catal. A: Gen.* 213 (2001) 279.
- [11] A. Bruckner, *Appl. Catal. A: Gen.* 200 (2000) 287.
- [12] C.T. Au, W. Hirsch and W. Hirschwald, *Surf. Sci.* 221 (1989) 113.
- [13] L.E. Briand, W.E. Farneth and I.E. Wachs, *Catal. Today* 62 (2000) 219.
- [14] O.R. de la Fuente, M. Borasio, P. Galletto, G. Rupprechter and H.J. Freund, *Surf. Sci.* 566–568 (2004) 740.
- [15] G.U. Kulkarni and C.N.R. Rao, *Topics Catal.* 22(3–4) (2003) 183.
- [16] M.H. Hu, S. Noda, T. Okubo, Y. Yamaguchi and H. Komiyama, *Appl. Surf. Sci.* 181 (2001) 307.
- [17] H.I. Kima, P. Frantza, S.V. Didziulis, L.C. Fernandez-Torres and S.S. Perry, *Surf. Sci.* 543 (2003) 103.
- [18] A.F. Lee, D.E. Gawthorpe, N.J. Hart and K. Wilson, *Surf. Sci.* 548 (2004) 200.
- [19] S. Damyanova et al, *J. Mol. Catal. A: Chem.* 142 (1999) 85.
- [20] M. Hara, M. Kawamura, J.N. Kondo, K. Domen and K. Maruya, *J. Phys. Chem.* 100 (1996) 14462.
- [21] C. Binet, M. Daturi and J.C. Lavalley, *Catal. Today* 50 (1999) 207.
- [22] L.J. Burcham, G. Deo, X.T. Gao, and I.E. Wachs, *Topics Catal.* 11 (2000) 85 (IR).
- [23] Notes, On the shift in the CH stratching bands of methoxy groups chemisorbed on metal oxides, *J. Catal.* 92 (1985) 173.
- [24] F. Ouyang and S. Yao, *J. Phys. Chem. B* 104 (2000) 11253.
- [25] M. Seman, J.N. Kondo, K. Domen and S.T. Oyama, *Chem. Lett.* (2002) 1082–1083.
- [26] X. Wang and I.E. Wachs, *Catal. Today* 96 (2004) 211.
- [27] G. Mul, M.A. Bañares, G. García Cortéz, B. van der Linden, S.J. Khatib and J.A. Moulijn, *Phys. Chem. Chem. Phys.* 5 (2003) 4378.
- [28] J.S. Chung, R. Miranda and C.O. Bennet, *J. Catal.* 114 (1988) 398.